J Mol Model (2013) 19:5601–5610
DOI 10.1007/s00894-013-2041-3

ORIGINAL PAPER

(Super)alkali atoms interacting with the σ electron cloud: a novel interaction mode triggers large nonlinear optical response of M@P_4 and M@C_3H_6 (M=Li, Na, K and Li_3O)

Xingang Zhao · Guangtao Yu · Xuri Huang · Wei Chen · Min Niu

Received: 27 August 2013 / Accepted: 21 October 2013 / Published online: 24 November 2013

Abstract Under high-level ab initio calculations, the geometrical structures and nonlinear optical properties of M@P_4 (M=Li, Na, K and Li_3O) and M@C_3H_6 (M=Li and Li_3O) were investigated; all were found to exhibit considerable first hyperpolarizabilities (18110, 1440, 22490, 50487, 2757 and 31776 au, respectively). The computational results revealed that when doping the (super)alkali atom M into the tetrahedral P_4 molecule, the original dual spherical aromaticity of the P_4 moiety is broken and new σ electron cloud is formed on the face of P_4 part interacting with the M atom. It was found that interaction of the (super)alkali atom with the σ electron cloud is a novel mode to produce diffuse excess electrons effectively to achieve a considerable β_0 value. Further, beyond the alkali atom, employing the superalkali unit can be a more effective approach to significantly enhance the first hyperpolarizability of the systems, due to the much lower vertical ionization potential. These results were further supported by the case of the (super)alkali atom interacting with the cyclopropane C_3H_6 molecule with its typical σ aromatic electron cloud. Moreover, the β_0 values of the M@P_4 series are nonmonotonic dependent on alkali atomic number, namely, 1440 au (M=Na)< 18110 au (Li)<22490 au (K), inferring that the distance between the alkali atom and the interacting surface with the σ electron cloud in P_4 is a crucial geometrical factor in determining their first hyperpolarizabilities. These intriguing findings will be advantageous for promoting the design of novel high-performance nonlinear optical materials.

Keywords First hyperpolarizability · P_4 molecule · Excess electron · Spherical aromaticity · σ Electron cloud · (Super)alkali atom

Introduction

In recent decades, starting from the earliest inorganic nonlinear optical (NLO) crystals, numerous investigations on designing high-performance NLO materials have focused the attention of experimental and theoretical researchers because of their extensive applications in optical and electro-optical devices etc. [1–5]. More and more innovatory structures with large NLO response have been proposed and synthesized theoretically and experimentally [6–23]. For example, it was revealed that organic molecules with a push–pull chromophore framework usually exhibit a considerable NLO response [6–11], in which a donor-π-acceptor scheme is constructed by linking the electron donor and acceptor at both ends of π-conjugated organic chains; NLO properties can be improved effectively by choosing appropriate donor/acceptor groups and changing the π-conjugated path. In particular, the type of π-conjugated bridge can play an important role in significantly increasing the first hyperpolarizability, as demonstrated by many investigated systems in which their π-conjugated paths are evolved from the simple linear structures (e.g. polyacetylene [6] and polyene [7]) to the more complicated electron-delocalized backbones (e.g. ladder-type polydiacetylenes derivatives with double π-conjugated chains [8]), even low-dimensional carbon nanostructures with π-conjugated characteristics (e.g. carbon nanotube (CNT) [9], graphene nanoribbon [10]), and the mixed π-conjugated

Electronic supplementary material The online version of this article (doi:10.1007/s00894-013-2041-3) contains supplementary material, which is available to authorized users.

X. Zhao · G. Yu (✉) · X. Huang · W. Chen (✉) · M. Niu
The State Key Laboratory of Theoretical and Computational Chemistry, Institute of Theoretical Chemistry, Jilin University, Changchun 130023, People's Republic of China
e-mail: yugt@jlu.edu.cn
e-mail: xychwei@gmail.com

bridge consisting of CNT and polyacetylene chain proposed very recently by our group [11].

Besides organic systems with a donor-π-acceptor arrangement, the metal-ligand compounds formed by incorporating transition metal into an organic complexant can also exhibit a large NLO response due to the occurrence of metal-to-ligand charge transfer (MLCT) [12–14]. For example, for ruthenium(II) complexes with substituted phenylpyridine ligand, the static first hyperpolarizability investigated by the experimental hyper-Rayleigh scattering technique is about 230 cm^5esu^{-1} [13]. Further investigations revealed that the category and number of the transition metal can significantly affect the NLO properties of metal-ligand complexes [15]. Moreover, several other species were also reported to possess considerably large NLO responses, for instance, octupolar organic molecules [16, 17] and X-type chiral π-conjugated oligomers, etc. [18]. Undoubtedly, the realization of these species can provide various outstanding candidates for the design of excellent NLO materials.

Different from the above mentioned structures, recent investigations have revealed that the electrides or alkalides containing the diffuse excess electron can present quite large first hyperpolarizability (β_0), in which the excess electron plays a crucial role in increasing the β_0 value, due to its existence resulting in the effective decrease of the excited energy [19–23]. Consequently, introducing the excess electron into these systems can become an effective approach to improve their NLO properties. At present, several different interacting modes have been proposed to produce the excess electron. First, via interaction of the alkali atom with the electron-withdrawing group, such as the H terminal of HCN molecule [19] and deficient-electron $B_{10}H_{14}$ basket [20], the *s* valence electron of the alkali atom can be pulled to form the diffuse excess electron. The excess electron can also be produced by means of pushing the *s* electron of the alkali atom under the action of the lone pairs of N or F atoms in complexants, such as in calix[4]pyrrole [21] and H-(CF2-CH2)3-H [22] systems, etc. Moreover, a new strategy has been proposed by our recent study, i.e., the excess electron can be introduced by the alkali atom interacting with the planar π-conjugated aromatic ring [23], which overcomes the bottleneck of the interacting modes reported previously that the excess electron is rather hard to be introduce into attractive carbon nanostructure and biomolecule systems with a π-conjugated aromatic ring. Obviously, the evolution of interacting modes to produce excess electron could be highly advantageous in realizing the design of new types of high-performance NLO materials.

Other than the planar aromaticity mentioned above, in this work, another kind of intriguing aromatic structure, spherical aromaticity, has also attracted our attention. Spherical aromaticity obeys the $2(N+1)^2$ rule [24–27]. Here, we investigated interaction of the alkali atom with the tetrahedral P_4 molecule—a typical paradigm with spherical aromaticity—in order to explore whether the excess electron can be achieved through this novel type of interacting manner and further leads to a considerable β_0 value. It is worth mentioning that a stable species of the lithium cation interacting with the P_4 molecule, named P_4Li^+, has been realized experimentally [28], in which the P_4 molecule maintains the structural integrity of the tetrahedron. Additionally, it was predicted theoretically that the P_4Li^+ species can be described as an intriguing "planetary system" [28], in which the Li^+ cation can move easily around the tetrahedral P_4 molecule along the paths/orbits connecting the points above the middle points of the P–P edges with the points above the center of the PPP faces. Besides the Li^+ cation, the interaction of another bare cation H^+ with the tetrahedral P_4 molecule was also investigated in theory and experiment [29], and it was found that different from the case of the analogous P_4Li^+, the H^+ cation can insert into one P–P bond in the P_4 molecule to form the stable and simple species P_4H^+ with a novel covalent P···H···P linkage. Moreover, many transition-metal complexes have also been employed to effectively functionalize the tetrahedral P_4 molecule [30, 31], and corresponding phosphorous-rich complexes can be achieved. For example, the Cp(CO)Co fragment can significantly alter the tetrahedral configuration of the P_4 molecule by cleaving the P–P bond; even a planar P_4 structure can be observed in complexes of $CpRh(CO)_2$ acting with P_4 [30]. Differently, the undistorted tetrahedral P_4 structure can be found in some complexes, such as $(P_4)AgAl[OC(CH_3)(CF_3)_2]_4$, due to the weak coordination between the P_4 molecule and Ag^+ cation [31]. Clearly, some progress has been made on investigations into phosphorous complexes based on the P_4 molecule. However, to the best of our knowledge, correlative reports on their NLO properties (e.g., the first hyperpolarizability) remain rather scarce.

In this study, we performed comprehensive ab initio computations to investigate the NLO properties of $M@P_4$ (M=Li, Na and K) systems with the new interacting mode of the alkali atom M acting with the interesting spherical aromatic P_4 molecule. Further, the correlative superalkali Li_3O unit was also considered, due to its much lower vertical ionization potential (VIP 3.40 eV) [32] than the corresponding alkali Li atom (5.39 eV) [32]. We will address mainly the following issues: (1) can the excess electron be produced as the alkali atom M interacting with the spherical aromatic P_4 molecule, and can its spherical aromaticity and tetrahedral structure be sustained in $M@P_4$? (2) If the diffuse excess electron is formed, can it cause the considerable first hyperpolarizability observed in $M@P_4$? (3) Are the β_0 values of $M@P_4$ (M=Li, Na and K) dependent on the atomic number of the alkali atom? (4) Can the superalkali Li_3O interacting with the P_4 molecule instead of the alkali atom further improve the NLO properties of the systems? By resolving these questions, this work can provide some new valuable insights

for the design of new high-performance NLO materials based on aromatic systems.

Computational methods

When a system is in a weak and homogeneous electric field, its energy can be written as: [33, 34]

$$E = E^0 - \mu_\alpha F_\alpha - \frac{1}{2}\alpha_{\alpha\beta}F_\alpha F_\beta - \frac{1}{6}\beta_{\alpha\beta\gamma}F_\alpha F_\beta F_\gamma \quad (1)$$

where E^0 is the molecular energy without the applied field; F_α is a component of the strength on the α direction of the applied electrostatic field; and μ_α, $\alpha_{\alpha\beta}$ and $\beta_{\alpha\beta\gamma}$ may be called components of the dipole, polarizability and first hyperpolarizability tensor, respectively.

The average electric dipole polarizability is defined as

$$\overline{\alpha} = \frac{1}{3}\left(\alpha_{xx} + \alpha_{yy} + \alpha_{zz}\right) \quad (2)$$

The first hyperpolarizability is defined as

$$\beta_i = \frac{3}{5}\left(\beta_{iii} + \beta_{ijj} + \beta_{ikk}\right) \quad i,j,k = x,y,z \quad (3)$$

$$\beta_0 = \sqrt{\left(\beta_x^2 + \beta_y^2 + \beta_z^2\right)} \quad (4)$$

In this work, the optimization and frequency analysis for all the geometrical structures was performed at the second-order Møller-Plesset perturbation (MP2) level with the 6-311G(d) basis set. The static first hyperpolarizabilities were computed by a finite field approach at the MP2/6-311+G(3df) level. The magnitude of the applied electric field was set as 0.001 a.u. for all systems studied. It is worth mentioning that the MP2 method has been applied extensively in investigations into NLO properties [35–38] due to its computational reliability, as reflected by the case that the computed results from the MP2 level can be close to those from more sophisticated correlation methods, such as coupled-cluster singles and doubles (CCSD) [39, 40] and the quadratic configuration interaction with single and double excitations (QCISD) [19, 23]. Here, we also considered the spin contamination of all computations on the geometrical optimization and NLO response. It was found that the corresponding $<S^2>$ values were in the range of 0.751 – 0.767, which is very close to the value 0.750 for the pure doublet state, indicating that the spin contamination is negligible and the computational results are reliable.

Moreover, time-dependent density functional theory (TD-DFT) calculations were performed at the Cam-B3LYP/6-311+G(3df) level to achieve the crucial excited states of the related structures. Note that the computed TD-DFT results based on Cam-B3LYP with the empirical exchange-correlation potential can be consistent with corresponding results based on the sampled B3PW91 and HSEH1PBE methods with the hybrid exchange-correlation potential. Detailed information has been provided in Electronic supplementary material. Moreover, differences in the dipole moments between the ground state and the crucial excited state were evaluated at the configuration interaction singles (CIS) level with the same basis set. The natural bond orbital (NBO) [41] population and nucleus independent chemical shift (NICS) values were computed at the B3LYP/6-311+G(3df) and MP2/6-311G(d) levels, respectively.

All computations in this study were carried out using the GAUSSIAN 09 program package [42].

Results and discussion

The geometries and NLO Properties of M@P_4 (M=Li, Na and K) and Li@C_3H_6

Initially, we considered all possible structures of the alkali atom M (M=Li, Na and K) interacting with the regular tetrahedral P_4 molecule, in which all three orientations, namely, peak-point, bond-point and face-point, are included. Among them, we achieved three face-point-based geometrical structures, all with real frequencies (Fig. 1), denoted as M@P_4 (M=Li, Na and K, respectively); the primary geometric parameters are listed in Table 1. All three M@P_4 molecules obtained has C_{3v} symmetry, where the alkali metal atom M (M=Li, Na and K) is located over one face (denoted by "f-P_4") of the tetrahedral P_4 molecule, and the distances (d) between the alkali atom M and the f-P_4 surface are 2.332, 2.965 and 3.812 Å for M=Li, Na and K, respectively. Obviously, the

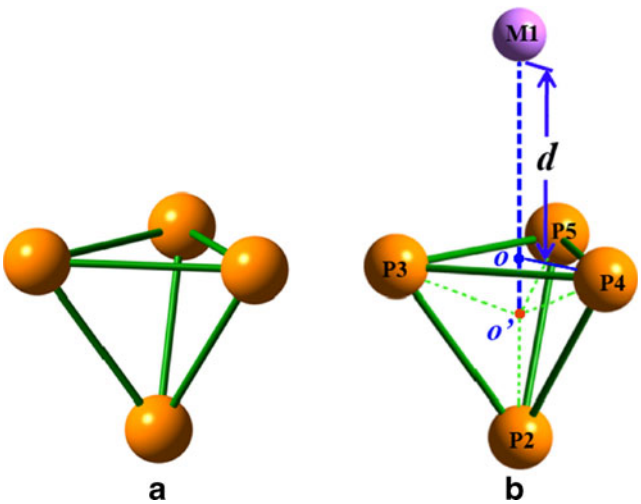

Fig. 1 Geometrical structures at the MP2/6-311G(d) level of **a** P_4 molecule and **b** M@P_4 (M=Li, Na and K)

Table 1 Main geometrical parameters of M@P_4 (M=Li, Na and K) molecules. Labels as in Fig. 1

Geometrical parameter		M@P_4			P_4
		Li	Na	K	
Distance(Å)	*d*	2.332	2.965	3.812	–
	P2-P3	2.236	2.206	2.204	2.204(2.205)[a]
	P3-P4	2.221	2.221	2.213	–
θ (M1P2P3) (°)		35.0	35.0	35.1	–
Symmetry		C_{3v}	C_{3v}	C_{3v}	T_h

[a] Average value of the single-crystal X-ray diffraction of the β-P_4 phase [46]

distance *d* increases along with the increase in the atomic number of alkali M. From the highest occupied molecular orbitals (HOMOs) of M@P_4 (M=Li, Na and K), we found that, under the action of the tetrahedral P_4 molecule, the *s* valence electron of the alkali metal atom M can be pushed out to become one diffuse excess electron, as illustrated in Fig. 2.

Subsequently, we intend to detailedly understand the nature of the interaction mode between the alkali atom M and the tetrahedral P_4 molecule to produce the diffuse excess electron, and whether spherical aromaticity can be still maintained in the P_4 part of the M@P_4 system after interacting with the alkali atom M. To address these intriguing issues, we first performed computations on the NBO populations of M@P_4 (M=Li, Na and K) and sole P_4 molecules, respectively. The tetrahedral P_4 molecule is well known to exhibit double spherical aromaticity in both the σ and π subsystems with the closed-shell nature [25], in which the σ system contains $2(N_\sigma+1)^2$ σ electrons (N_σ=2) and is composed of a cluster *s* orbital, three degenerate cluster *p* orbitals, and two sets of cluster *d* orbitals, while the π system contains $2(N_\pi+1)^2$ π electrons (N_π=0), as shown in Fig. 3. Comparing the corresponding molecular orbitals between the M@P_4 (Li, Na and K) and P_4 systems (Fig. 3) revealed that doping the alkali atom M can break the dual spherical aromaticity corresponding to

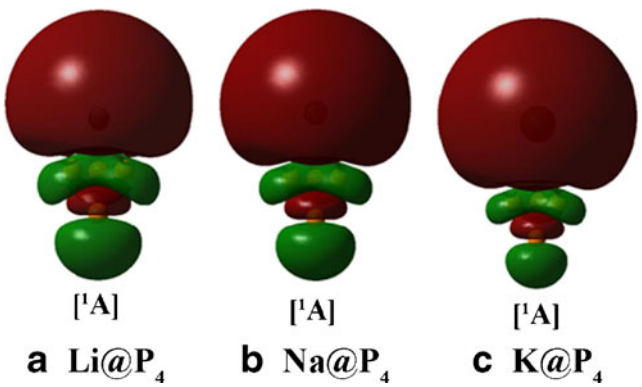

Fig. 2 Highest occupied molecular orbitals (HOMO) and the corresponding orbital symmetries (in brackets) of M@P_4 (M=Li, Na and K) molecules at the MP2/6-311G(d) level

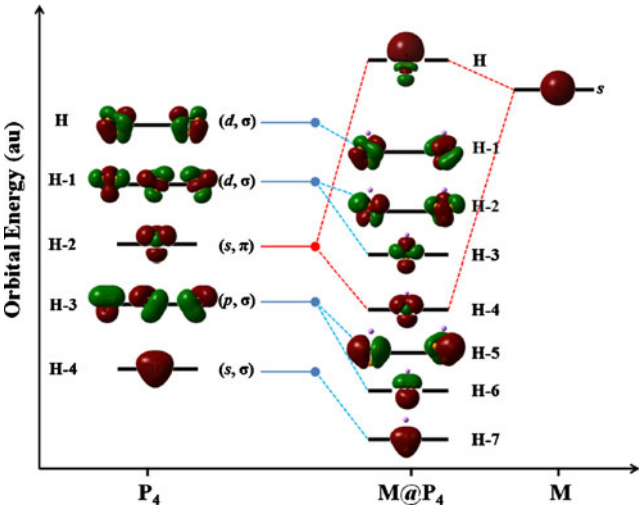

Fig. 3 Relationship of molecular/atomic orbitals of the tetrahedral P_4 molecule (*left*), M atom (*right*) and M@P_4 (M=Li, Na and K) compounds (*middle*). *H* indicates the highest occupied molecular orbital with respect to the Hartree-Fock orbital based on the optimized geometries at the MP2/6-311G(d) level

the σ and π subsystems in the tetrahedral P_4 molecule, where the degeneracy of the original three-cluster *p*/*d* orbitals is broken in the σ subsystem, while the interaction of the HOMO-2 orbital related to the π subsystem of the P_4 molecule with the *s* atomic orbital of the M atom leads to the corresponding HOMO and HOMO-4 orbitals in M@P_4 (M=Li, Na and K), with bonding and anti-bonding characteristics, respectively. By analyzing the constituents of the HOMO of M@P_4 (M=Li, Na and K), it was found that, for all P_4 parts in the three systems, the electron cloud that is distributed on three P atoms, constituting the *f*-P_4 interacting surface, originates mainly from their *s* orbitals, which leads to the formation of a σ electron cloud on the *f*-P_4 surface, while the *p* orbital contributes mainly to the electron cloud on the remaining P atom (Fig. 2).

To further confirm the broken spherical aromaticity of the P_4 part, and the existence of the σ electron cloud in the *f*-P_4 surface of M@P_4 (M=Li, Na and K), we performed a computation on the scanning NICS values (proposed by Schleyer and co-workers [43]) near the *f*-P_4 surface, which can reflect the aromaticity of a molecule based on the negative values of the computed magnetic shielding. By comparing all calculated NICS values near the *f*-P_4 surface, the most negative NICS value was found at the center of the *f*-P_4 surface for all three systems M@P_4 (M=Li, Na and K), which is different from the nonexistence of the most negative NICS value at the center of the *f*-P_4 surface for the sole P_4 molecule (Fig. 4). The different location of the most negative NICS value between P_4 and M@P_4 systems further supports the claim mentioned above, namely, the spherical aromaticity of P_4 molecule was broken and a σ electron cloud in the *f*-P_4 surface was formed simultaneously in M@P_4. As shown in Fig. 2, under the action of the σ electron cloud, the *s* electron of the alkali atom M is

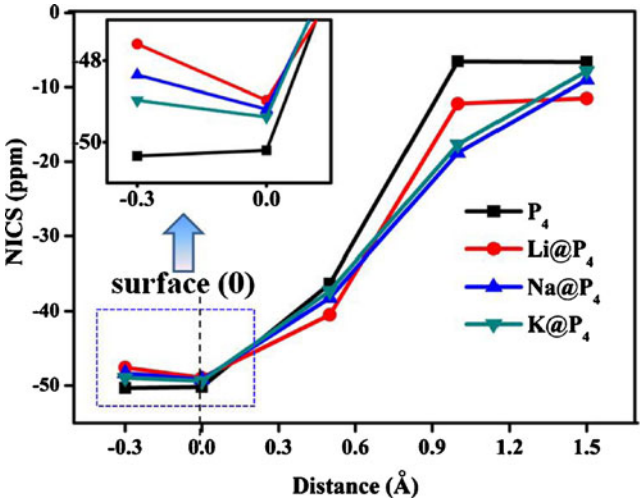

Fig. 4 Scanning curves of nucleus independent chemical shift (NICS) values in M@P_4 (M=Li, Na and K) and P_4 molecules. *Surface (0)* represents the interacting surface (*f*-P_4) of M@P_4 or one surface of P_4

pushed out to form the diffuse excess electron in M@P_4 (M=Li, Na and K), which is considered a novel interaction mode producing the excess electron.

Previous studies have revealed that the diffuse excess electron can usually cause a considerable NLO response [19–23]. Indeed, our computed results showed that the M@P_4 (M=Li, Na and K) molecules can exhibit very large first hyperpolarizabilities (β_0=18110, 1440 and 22490 a.u.) as well as polarizabilities (α=303, 294 and 384 a.u. for M=Li, Na and K, respectively), compared with the sole P_4 molecule (β_0=0 and α=92 a.u.).

To understand why the M@P_4 (M=Li, Na and K) system has much larger β_0 values than the sole P_4 molecule, we can employ the following two-level expression [44]:

$$\beta_0 \propto \Delta\mu \cdot f_0 / \Delta E^3 \quad (5)$$

where ΔE, f_0 and $\Delta\mu$ are the crucial transition energy, the largest oscillator strength, and the difference of dipole moment between the ground state and the crucial excited state (the excited state with the largest oscillator strength), respectively. In the two-level model, the third power of the transition energy is inversely proportional to the β_0 value. Therefore, the low transition energy is the crucial factor in achieving large first hyperpolarizabilities. Accordingly, the ΔE value is primarily considered in the following discussion on first hyperpolarizabilities.

TD-DFT computations were performed to obtain the crucial excited states of the M@P_4 (M=Li, Na and K) and P_4 molecules, respectively. From Table 2 and Fig. 5, it can be seen that the electron involved in the crucial excited states of the M@P_4 (M=Li, Na and K) species is from their HOMO orbitals, which are composed mainly of the diffuse *s* orbital of the Li, Na or K atom. Clearly, under the action of the σ electron cloud reformed in the new M@P_4 species, the *s* electron of the alkali atom M is pushed out into a highly diffuse orbital and becomes the excess electron, which is easily excited due to the weaker interaction with the Li/Na/K core. Therefore, it is reasonable to expect that the M@P_4 (M=Li, Na and K) system has a much smaller crucial transition energy ΔE than the P_4 molecule. Indeed, as confirmed by the computed TD-DFT results, the transition energy for the P_4 molecule is up to 7.21 eV, whereas the corresponding values can decrease sharply to 1.65, 1.98, and 1.50 eV for Li@P_4, Na@P_4 and K@P_4, respectively, resulting in quite large β_0 values for these M@P_4 systems, according to two-level expression.

Obviously, the above results reveal a new effective approach to achieve a large β_0 value through the alkali atom interacting with the σ electron cloud to produce the diffuse excess electron. In order to further confirm this novel interaction mode, we took the cyclopropane C_3H_6 molecule with σ-aromatic characteristic as an example to investigate interaction of the alkali Li atom with the σ electron cloud, and wonder whether the excess electron could be also produced to cause a large β_0 value in the Li@C_3H_6 system. As shown in Fig. 6a, the Li@C_3H_6 structure has C_{3v} symmetry, where the Li atom is located over the cyclopropane molecule at a distance of 4.539 Å. Intriguingly, a similar phenomena can be observed, i.e., the *s* electron of the Li atom can also be pushed out to form diffuse excess electron under the action of the σ electron-cloud of the cyclopropane molecule (Fig. 6a), and a large β_0 value (β_0=2757 au) was realized in Li@C_3H_6, in contrast to the sole cyclopropane molecule (β_0=0 a.u.). Clearly, this further supports the case that the alkali atom interacting with the σ electron cloud is a new effective mode to introduce the excess electron and obtain a large NLO response, which will be advantageous to facilitate the design of new types of high-performance NLO materials.

Nonmonotonic dependency of the first hyperpolarizabilities of M@P_4 (M=Li, Na and K)

The computational results (Table 2) revealed the nonmonotonic dependency of the β_0 values of the M@P_4 species on the alkali atomic number: 1440 a.u. (M=Na)<18110 a.u. (Li)<22490 a.u. (K), although the VIP value of the alkali atom M decreases with increasing alkali atomic number, and it is anticipated that the *s* valence electron of the heavier M atom can be more easily pushed out to form a more diffuse excess electron and the resulting larger β_0 value may be achieved.

We next asked, what is the reason for the occurrence of the unmonotonic β_0 dependency of the M@P_4? This can be attributed mainly to the fact that, besides the influence of the VIP value of the alkali atom, the distance (*d*) between the M atom and the *f*-P_4 surface with the σ electron cloud also plays an important role, similar to the case of the studied M@pyrrole (M=Li, Na and K) systems with the alkali atom

Table 2 Polarizability ($\bar{a}$), first hyperpolarizability (β_0), transition energy (ΔE), difference in dipole moment between the ground state and the crucial excited state ($\Delta\mu$), oscillator strength (f_0) and composition of the crucial transition state of M@P_4 (M=Li, Na, K and Li_3O) and P_4 molecules. The estimated β_0 value ($\Delta\mu f_0/\Delta E^3$) was obtained under two-level expression

Properties	M@P_4				P_4
	Li	Na	K	Li_3O[a]	
$\bar{a}$ (a.u.)	303	294	384	396	92
β_0 (a.u.)	18,110	1,440	22,490	50,487	0
$\Delta\mu$ (Debye)	2.799	0.716	1.706	10.478	1.201
ΔE (eV)	1.65	1.98	1.50	1.33	7.21
f_0	0.3409	0.4468	0.4428	0.1389	0.2432
Estimated β_0 (a.u.)	1,683	327	1,773	4,901	6
Composition of the crucial transition state	H→L+2[b]	H→L+1	H→L+1	H→L+1	H-3→L H-2→L H-2→L+1 H→L+1

[a] β_0 value at the coupled-cluster singles and doubles (CCSD) level with basis set 6-311 +G(3df) for Li_3O and 6-31G(d) for P atoms, respectively

[b] *H* Highest occupied molecular orbital (HOMO), *L* lowest unoccupied molecular orbital (LUMO)

M interacting with the planar aromatic π electron cloud [23]. Our computed result shows that the distance (d=2.965 Å) between the alkali Na atom and the f-P_4 surface in Na@P_4 approximates the middle value between the corresponding distances of Li@P_4 (2.332 Å) and K@P_4 (3.812 Å), which can lead to a situation in which the interaction between the Na atom and the f-P_4 surface with the σ electron cloud is weakest in these three structures, since the atom radius of the Na atom (2.230 Å) is closer to that of the Li atom (2.050 Å) and both are much smaller than that of the K atom (2.770 Å). As a result, the excess electron formed from the *s* valence electron of the Na atom can be less diffuse than that of the Li/K atom in the M@P_4 series, in spite of the decrease of the VIP value of M with increasing alkali atomic number. Usually, the more diffuse excess electron will be easier to excite. Indeed, the transition energy ΔE in the crucial excited state of Na@P_4 is the largest among the M@P_4 series, namely, 1.94 eV (M=Na)>1.73 eV (Li)>1.48 eV (K), as revealed by our computed TD-DFT results.

Consequently, according to the two-level expression, we conclude that the order of corresponding β_0 values for M@P_4 (Li, Na, and K) is not monotonically dependent on the alkali metal atomic number, namely, 1440 au (Na@P_4)<18110 au (Li@P_4)<22490 au (K@P_4) (Fig. 7). It is worth mentioning that their β_0 values estimated using the correlative $\Delta E, f_0$ and $\Delta\mu$ parameters under the two-level formula can also exhibit a trend similar to the corresponding computed β_0 values (inset in Fig. 7).

Clearly, besides the VIP of the alkali atom M itself, the geometrical distance d between M and the σ electron cloud is also a crucial factor that can significantly change the β_0 values of M@P_4 (M=Li, Na, and K) series by affecting their corresponding ΔE values. This is further supported by the computed results on the curves of the ΔE and β_0 as a function of the distance d (Fig. 8), i.e., as the distance d of the three

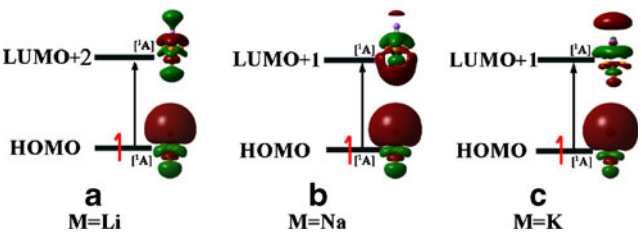

Fig. 5 Crucial transition states and symmetries of transition molecule orbitals (in *brackets*) of the M@P_4 (M=Li, Na and K) molecules based on TD-DFT results. The *red arrow* indicates excess electron in the HOMO

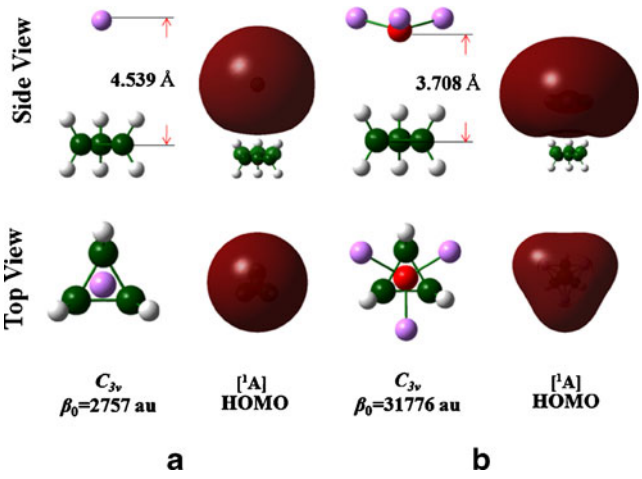

Fig. 6 Top and side views of the geometrical structures, the corresponding HOMOs and their orbital symmetries (in brackets) of **a** Li@C_3H_6 and **b** Li_3O@C_3H_6 molecules, as well as their respective symmetries, interacting distances (d) and β_0 values

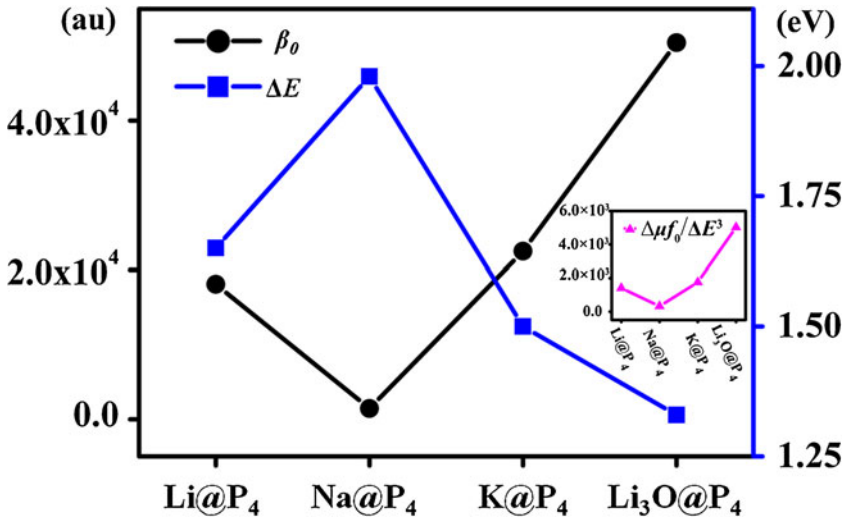

Fig. 7 Curves of the first static hyperpolarizabilities (β_0, *black*) and the corresponding transition energies (ΔE, *blue*) of M@P_4 (M=Li, Na, K and Li_3O) molecules. *Inset* Estimated β_0 values under the two-level expression (*pink*)

molecules increases, the corresponding ΔE values increase and the β_0 values decrease.

NLO properties of $Li_3O@P_4$ and $Li_3O@C_3H_6$

Considering that superalkali compounds can exhibit much lower VIP values—for example, the VIP value of Li_3O (3.40 eV)[32] is lower than the parallel alkali Li atom (5.39 eV)—in this study we sampled the Li_3O molecule replacing the Li atom in Li@P_4 and investigated the first hyperpolarizability of the $Li_3O@P_4$ system, in order to understand whether employing a superalkali unit can further effectively improve the NLO response of the system. We highly expected that $Li_3O@P_4$ can possess a much larger first hyperpolarizability, given that the lower VIP of the employed Li_3O unit may result in a more diffused excess electron, further achieving a larger β_0 value.

In this work, all possible $Li_3O@P_4$ configurations were considered, and only one geometric structure (face to face type) with all real frequencies was finally obtained, as illustrated in Fig. 9. After interacting with the P_4 molecule, the

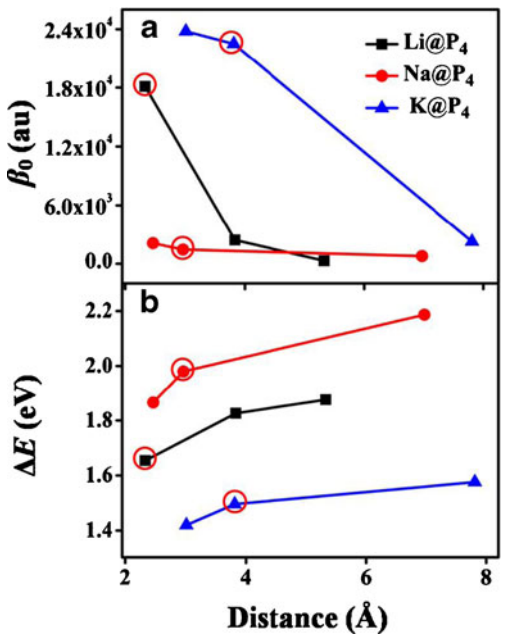

Fig. 8 Curves of **a** first hyperpolarizability β_0 and **b** transition energy ΔE as a function of the distance d between the interacting surface f-P_4 (P3-P4-P5 in Fig. 1) and the alkali metal atom **M** in the M@P_4 (M=Li, Na and K) species. The *points in red circles* coincide with the ΔE or β_0 values of the fully optimized geometries of M@P_4 (M=Li, Na and K)

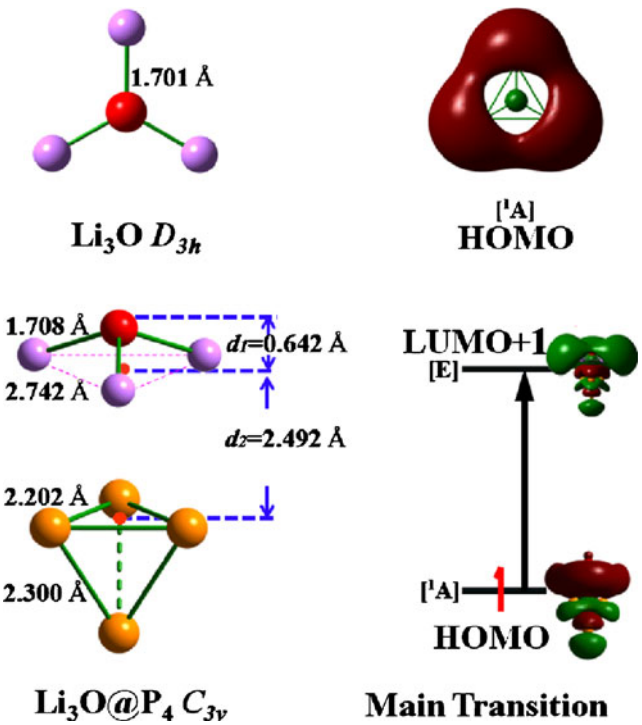

Fig. 9 Geometrical structures of Li_3O and $Li_3O@P_4$, the HOMO orbital of Li_3O, and the main transition state of $Li_3O@P_4$ based on TD-DFT results. The symmetries of the molecular orbitals are labeled in *brackets*

Li_3O unit was found to change from a planar to an umbrella shape with a distance of 0.642 Å between the oxygen atom and the plane formed by the three Li atoms (labeled as *f*-Li_3) in the $Li_3O@P_4$, yet the distance (2.492 Å) between the *f*-Li_3 in Li_3O and the *f*-P_4 surface is close to that (2.332 Å) between the Li atom and *f*-P_4 in $Li@P_4$, and similar to the case of the $Li@P_4$, the P–P bond lengths in the P_4 part of $Li_3O@P_4$ also exhibit only a slight change within the range of 0.006–0.096 Å, compared with the sole P_4 molecule. Besides, it is more intriguing that the σ electron cloud can also be observed in the *f*-P_4 surface of $Li_3O@P_4$ and, under the action of this electron cloud, the valence electron of the Li_3O unit (HOMO in Fig. 9) can be pushed out to form the highly diffuse excess electron. As expected, the resulting β_0 value of $Li_3O@P_4$ is then considerably larger at 50487 a.u., which is much larger than the β_0 values of $Li@P_4$ (18110), $Na@P_4$ (1440), $K@P_4$ (22490 a.u.). The β_0 trend between the superalkali $Li_3O@P_4$ and alkali $M@P_4$ (M=Li, Na and K) systems is well consistent with those of their ΔE values (1.33 eV for $Li_3O@P_4$ and 1.65, 1.98 and 1.50 eV for $M@P_4$, M=Li, Na and K) and their estimated β_0 values under two-level expression (4091 a.u. for $Li_3O@P_4$ and 1683, 327 and 1773 a.u. for $M@P_4$, M=Li, Na and K, respectively), as shown in Fig. 7.

Undoubtedly, employing a superalkali unit to interact with the σ electron cloud is a more effective approach to trigger large β_0 values. Further, this result is also supported by the case of the superalkali Li_3O unit interacting with the cyclopropane C_3H_6 molecule with σ aromaticity [45]. As shown in Fig. 6b, in $Li_3O@C_3H_6$ molecule with C_{3v} symmetry, the Li_3O is located over the C_3H_6 ring at a distance of 3.708 Å. Similar to $Li@C_3H_6$, under the interaction of the σ electron cloud of the cyclopropane molecule, the outer electron of Li_3O is pushed out to form the excess electron, which endows $Li_3O@C_3H_6$ with the considerably large β_0 value of 31776 a.u., almost 11 times larger than that of $Li@C_3H_6$ (Fig. 6a).

Conclusions

In this work, we performed a systematic theoretical investigation on the geometrical structures and first hyperpolarizabilities of the $M@P_4$ (M=Li, Na, K and Li_3O) and $M@C_3H_6$ (M=Li and Li_3O) series. Compared with single P_4 or C_3H_6 molecules, these new compounds exhibit considerable first hyperpolarizabilities, which are 18110, 1440, 22490, 50487 a.u. for $Li@P_4$, $Na@P_4$, $K@P_4$, $Li_3O@P_4$, and 2757, 31776 a.u. for $Li@C_3H_6$ and $Li_3O@C_3H_6$, respectively.

Our computed results revealed that doping the (super)alkali atom M can break the original double spherical aromaticity of the tetrahedral P_4 molecule, and the σ electron cloud is formed at the interacting surface of the P_4 moiety with the M atom in the $M@P_4$ series. Upon interaction with the newly formed σ electron cloud, the valence electron of the (super)alkali atom is pushed out to produce a diffuse excess electron. A similar case of a (super)alkali atom M interacting with the σ electron cloud to introduce an excess electron can also be observed in $M@C_3H_6$ (M=Li and Li_3O) systems, where the C_3H_6 cyclic molecule possesses an intrinsic σ aromatic electron cloud.

In conclusion, we propose a new and effective strategy through the (super)alkali atom interacting with the σ electron cloud to form a diffuse excess electron, which can lead to a quite large first hyperpolarizability. Beyond the alkali atoms, doping the superalkali atom can enhance the first hyperpolarizability of the systems more effectively because of the much lower VIP value. Moreover, it was found that the distance *d* between the alkali atom M and the interacting surface with the σ electron cloud can also play a crucial role in affecting the β_0 values of the $M@P_4$ (M=Li, Na and K) series, as reflected by the β_0 nonmonotonic dependency on the alkali atomic number, i.e., 1440 a.u. (M=Na)<18110 a.u. (Li)<22490 a.u. (K). Undoubtedly, these intriguing findings will be useful for advancing the design of novel high-performance NLO materials.

Acknowledgments This work was supported by National Natural Science Foundation of China (21103065, 21373099, 21073075 and 21173097), National Basic Research Program of China (973 Program) (2012CB932800), and the Ministry of Education of China (20110061120024 and 20100061110046). We acknowledge the High Performance Computing Center (HPCC) of Jilin University for supercomputer time.

References

1. Lacroix PG (2001) Second-order optical nonlinearities in coordination chemistry: the case of bis(salicylaldiminato)metal Schiff base complexes. Eur J Inorg Chem 2001:339–348
2. Marder SR (2006) Organic nonlinear optical materials: where we have been and where we are going. Chem Commun 2:131–134
3. Zhang C, Song YL, Wang X (2007) Correlations between molecular structures and third-order non-linear optical functions of heterothiometallic clusters: a comparative study. Coordin Chem Rev 251:111–141
4. Batista RMF, Costa SPG, Belsley M, Lodeiro C, Raposo MMM (2008) Synthesis and characterization of novel (oligo) thienylimidazo-phenanthrolines as versatile π-conjugated systems for several optical applications. Tetrahedron 64:9230–9238
5. Suresh S, Arivuoli D (2012) Nanomaterials for nonlinear optical (NLO) appilcations: a review. Rev Adv Mater Sci 30:243–253
6. Morley JO, Docherty VJ, Pugh D (1987) Non-linear optical properties of organic molecules. Part 2. Effect of conjugation length and molecular volume on the calculated hyperpolarisabilities of polyphenyls and polyenes. J Chem Soc Perkin Trans II:1351–1355
7. Blanchard-Desce M, Alain V, Bedworth PV, Marder SR, Fort A, Runser C, Barzoukas M, Lebus S, Wortmann R (1997) Large quadratic hyperpolarizabilities with donor–acceptor polyenes exhibiting optimum bond length alternation: correlation between structure and hyperpolarizability. Chem Eur J 3:1091–1104
8. Chen W, Yu GT, Gu FL, Aoki Y (2009) Investigation on nonlinear optical properties of ladder-structure polydiacetylenes derivatives by using the elongation finite-field method. Chem Phys Lett 474:175–179

9. Xiao D, Bulat FA, Yang W, Beratan DN (2008) A donor–nanotube paradigm for nonlinear optical materials. Nano Lett 8:2814–2818
10. Zhou ZJ, Li XP, Ma F, Liu ZB, Li ZR, Huang XR, Sun CC (2011) Exceptionally large second–order nonlinear optical response in donor–graphene nanoribbon–acceptor systems. Chem Eur J 17:2414–2419
11. Yu GT, Zhao XG, Niu M, Huang XR, Zhang H, Chen W (2013) Constructing a mixed p-conjugated bridge: a simple and effective approach to realize a large first hyperpolarizability in carbon nanotube-based systems. J Mater Chem C 1:3833–3841
12. Buey J, Coco S, Díez L, Espinet P, Martín-Alvarez JM, Miguel JA, García-Granda S, Tesouro A, Ledoux I, Zyss J (1998) Synthesis and second-order nonlinear optical properties of new palladium (II) and platinum (II) Schiff-base complexes. Organometallics 17:1750–1755
13. Labat L, Lamère JF, Sasaki I, Lacroix PG, Vendier L, Asselberghs I, Pérez-Moreno J, Clays K (2006) Synthesis, crystal structure, and second-order nonlinear optical properties of ruthenium(II) complexes with substituted bipyridine and phenylpyridine ligands. Eur J Inorg Chem 2006:3105–3113
14. Espinet P, Miguel JA, Martín-Alvarez JM, Villacampa B (2010) Synthesis, crystal structure and second-order nonlinear optical properties of the trinuclear palladium orthometalated complex [(μ_3-S)(μ_3-OH)Pd_3(C^N)$_3$] (HC6^N=p-Bu^n_2N–C_6H_4–CH=N–C_6H_4–NO_2-p). J Organomet Chem 695:437–440
15. Bella SD (2001) Second-order nonlinear optical properties of transition metal complexes. Chem Soc Rev 30:355–366
16. Maury O, Viau L, Senechal K, Corre B, Guegan JP, Renouard T, Ledoux I, Zyss J, Bozec LH (2004) Synthesis, linear and quadratic–nonlinear optical properties of octupolar D3 and D2d bipyridyl metal complexes. Chem Eur J 10:4454–4466
17. Lee SH, Park JR, Jeong MY, Kim HM, Li SJ, Song J, Ham S, Jeon SJ, Cho BR (2006) First hyperpolarizabilities of 1,3,5-tricyanobenzene derivatives: origin of larger β values for the octupoles than for the dipoles. Chem Phys Chem 7:206–212
18. Cornelis D, Franz E, Asselberghs I, Clays K, Verbiest T, Koeckelberghs G (2011) Interchromophoric interactions in chiral X-type π-conjugated oligomers: a linear and nonlinear optical study. J Am Chem Soc 133:1317–1327
19. Chen W, Li ZR, Wu D, Li RY, Sun CC (2005) Theoretical investigation of the large nonlinear optical properties of $(HCN)_n$ clusters with Li atom. J Phys Chem B 109:601–608
20. Muhammad S, Xu HL, Liao Y, Kan Y, Su ZM (2009) Quantum mechanical design and structure of the Li@ $B_{10}H_{14}$ basket with a remarkably enhanced electro-optical response. J Am Chem Soc 131:11833–11840
21. Chen W, Li ZR, Wu D, Li Y, Sun CC, Gu FL (2005) The structure and the large nonlinear optical properties of Li@Calix[4]pyrrole. J Am Chem Soc 127:10977–10981
22. Xu HL, Li ZR, Wu D, Wang BQ, Li Y, Gu FL, Aoki Y (2007) Structures and large NLO responses of new electrides: Li-doped fluorocarbon chain. J Am Chem Soc 129:2967–2970
23. Yu GT, Huang XR, Chen W, Sun CC (2011) Alkali metal atom-aromatic ring: a novel interaction mode realizes large first hyperpolarizabilities of M@AR (M=Li, Na, and K, AR = pyrrole, indole, thiophene, and benzene). J Comput Chem 32:2005–2011
24. Hirsch A, Chen ZF, Jiao HJ (2000) Spherical aromaticity in Ih symmetrical fullerenes: the $2(N+1)^2$ rule. Angew Chem Int Ed 39:3915–3917
25. Hirsch A, Chen ZF, Jiao HJ (2001) Spherical aromaticity of inorganic cage molecules. Angew Chem Int Ed 40:2834–2838
26. Chen ZF, Jiao HJ, Hirsch A, Schleyer PR (2002) Spherical homoaromaticity. Angew Chem Int Ed 41:4309–4312
27. Reiher M, Hirsch A (2003) From rare gas atoms to fullerenes: spherical aromaticity studied from the point of view of atomic structure theory. Chem Eur J 9:5442–5452
28. Abboud JLM, Alkorta I, Davalos JZ, Gal JF, Herreros M, Maria PC, Mo O, Molina MT, Notario R, Yanez M (2000) The $P_4\cdots Li^+$ ion in the gas phase: a planetary system. J Am Chem Soc 122:4451–4454
29. Abboud JLM, Herreros M, Notario R, Esseffar M, MÓ O, Yáñez M (1996) A new bond from an old molecule: formation, stability, and structure of P_4H^+. J Am Chem Soc 118:1126–1130
30. Scherer OJ (1990) Complexes with substituent–free acyclic and cyclic phosphorus, arsenic, antimony, and bismuth ligands. Angew Chem Int Ed Engl 29:1104–1122
31. Krossing I, van Wüllen L (2002) Superweak complexes of tetrahedral P_4 molecules with the silver cation of weakly coordinating anions. Chem Eur J 8:700–711
32. Rehm E, Boldyrev AI, Schleyer PR (1992) Ab initio study of superalkalis. First ionization potentials and thermodynamic stability. Inorg Chem 31:4834–4842
33. Buckingham AD (1967) The effects of collisions on molecular properties. Adv Chem Phys 12:107–142
34. Mclean AD, Yoshimine M (1967) Theory of molecular polarizabilities.J. Chem Phys 47:1927–1935
35. Li Y, Li ZR, Wu D, Li RY, Hao XY, Sun CC (2004) An ab initio prediction of the extraordinary static first hyperpolarizability for the electron-solvated cluster (FH)2{e}(HF). J Phys Chem B 108:3145–3148
36. Li ZJ, Li ZR, Wang FF, Luo C, Ma F, Wu D, Wang Q, Huang XR (2009) A dependence on the petal number of the static and dynamic first hyperpolarizability for electride molecules: many-petal-shaped Li-doped cyclic polyamines. J Phys Chem A 113:2961–2966
37. Suponitsky KY, Liao Y, Masunov AE (2009) Electronic hyperpolarizabilities for donor–acceptor molecules with long conjugated bridges: calculations versus experiment. J Phys Chem A 113:10994–11001
38. Ma F, Li ZR, Xu HL, Li ZJ, Li ZS, Aoki Y, Gu FL (2008) Lithium salt electride with an excess electron pair—a class of nonlinear optical molecules for extraordinary first hyperpolarizability. J Phys Chem A 112:11462–11467
39. Soscún H, Castellano O, Bermúdez Y, Toro-Mendoza C, Marcano A, Alvarado Y (2002) Linear and nonlinear optical properties of pyridine N-oxide molecule. J Mol Struct THEOCHEM 592:19–28
40. Sekino H, Maeda Y, Kamiya M, Hirao K (2007) Polarizability and second hyperpolarizability evaluation of long molecules by the density functional theory with long-range correction. J Chem Phys 126:014107
41. Glendening ED, Reed AE, Carpenter JE, Weinhold F (1996) NBO Version 3.1. Theoretical Chemistry Institute, University of Wisconsin, Madison
42. Frisch MJ, Trucks GW, Schlegel HB, Scuseria GE, Robb MA, Cheeseman JR, Scalmani G, Barone V, Mennucci B, Petersson GA, Nakatsuji H, Caricato M, Li X, Hratchian HP, Izmaylov AF, Bloino J, Zheng G, Sonnenberg JL, Hada M, Ehara M, Toyota K, Fukuda R, Hasegawa J, Ishida M, Nakajima T, Honda Y, Kitao O, Nakai H, Vreven T, Montgomery JA Jr, Peralta JE, Ogliaro F, Bearpark M, Heyd JJ, Brothers E, Kudin KN, Staroverov VN, Keith T, Kobayashi R, Normand J, Raghavachari K, Rendell A, Burant JC, Iyengar SS, Tomasi J, Cossi M, Rega N, Millam JM, Klene M, Knox JE, Cross JB, Bakken V, Adamo C, Jaramillo J, Gomperts R, Stratmann RE, Yazyev O, Austin AJ, Cammi R, Pomelli C, Ochterski JW, Martin RL, Morokuma K, Zakrzewski VG, Voth GA, Salvador P, Dannenberg JJ, Dapprich S, Daniels AD, Farkas O, Foresman JB, Ortiz JV, Cioslowski J, Fox DJ (2010) Gaussian 09, Revision B.01. Gaussian, Inc, Wallingford
43. Schleyer PR, Maerker C, Dransfeld A, Jiao H, Eikema-Hommes NJR (1996) Nucleus-independent chemical shifts: a simple and efficient aromaticity probe. J Am Chem Soc 118:6317–6318

44. Kanis DR, Ratner MA, Marks TJ (1994) Design and construction of molecular assemblies with large second-order optical nonlinearities. Quant Chem Asp Chem Rev 94:195–242
45. Cremer D, Gauss J (1986) Theoretical determination of molecular structure and conformation. 20. Reevaluation of the strain energies of cyclopropane and cyclobutane carbon-carbon and carbon-hydrogen bond energies, 1,3 interactions, and .sigma.-aromaticit. J Am Chem Soc 108:7467–7477
46. Simon A, Borrmann H, Horakh J (1997) On the polymorphism of white phosphorus. Chem Ber 130:1235–1240